DE LA RECHERCHE À L'INDUSTRIE

High-order fluid-structure coupling for 2D Finite Volume Lagrange-Remap schemes

Gautier Dakin[1] Bruno Després[2] Stéphane Jaouen[1]

[1]CEA, DAM, DIF, F-91297 Arpajon, France

[2]Université Pierre et Marie Curie, LJLL, Paris, France

SHARK-FV 2018 CONFERENCE

SHARING HIGHER-ORDER ADVANCED RESEARCH KNOW-HOW ON FINITE VOLUME

Porto, Portugal
May 21-25, 2018

Outlines

1. Context
2. Boundary conditions discretization for linear hyperbolic systems
   - Inverse Lax–Wendroff procedure
   - Scheme stability with boundary conditions discretization
3. Boundary conditions discretization for compressible hydrodynamocs
   - Inverse Lax–Wendroff for $\rho_0 = 1$, $m = 2$, $n = 1$
   - Existence and uniqueness of the reconstruction in the general case
4. Fluid - rigid body coupling
   - Properties and spatial discretization of rigid bodies
   - Fluid - structure coupling scheme

Context

Consider Ω_f as the fluid domain and Ω_s as the solid one. Define Γ as the border between both domains. Denote $\mathbf{u_f}$ the fluid velocity, $\mathbf{u_s}$ the solid one and also $\underline{\sigma}_f$ and $\underline{\sigma}_s$ the fluid and solid constraints tensors. Let $\mathbf{n}_\Gamma$ be the normal outward Γ.

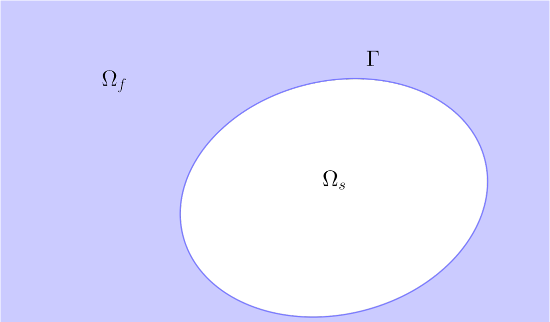

Boundary conditions on the border Γ writes

$$\boxed{\mathbf{u_f} \cdot \mathbf{n}_\Gamma = \mathbf{u_s} \cdot \mathbf{n}_\Gamma, \quad \underline{\sigma}_f \cdot \mathbf{n}_\Gamma = \underline{\sigma}_s \cdot \mathbf{n}_\Gamma, \quad \text{sur} \quad \Gamma.} \tag{1}$$

Inside $\Omega_f \subset \mathbb{R}^2$, consider the Euler system of equations[1] which writes

$$\begin{cases} \partial_t \rho + \nabla.(\rho \mathbf{u}) & = 0, \\ \partial_t(\rho \mathbf{u}) + \nabla.(\rho \mathbf{u} \otimes \mathbf{u} + p\underline{\mathbf{I}}) & = 0, \\ \partial_t(\rho e) + \nabla.(\rho e \mathbf{u} + p \mathbf{u}) & = 0, \\ p & = EOS(\rho, u, e) \end{cases} \tag{2}$$

with variables ρ, p, $\mathbf{u}$, e for the density, the pressure, the velocity, and the total energy. System is closed using the equation of state EOS.

The schemes used usually inside the laboratory are very high-order accurate finite volume Lagrange remap schemes based on cartesian grids[2][3][4].

[1] E. Godlewski and P.-A. Raviart. *Numerical approximation of hyperbolic systems of conservation laws*. Vol. 118. Springer Science & Business Media, 2013.

[2] F. Duboc et al. "High-order dimensionally split Lagrange-remap schemes for compressible hydrodynamics". *C. R. Acad. Sci. Paris, Ser. I* 348 (2010), pp. 105–110.

[3] M. Wolff. "Mathematical and numerical analysis of the resistive magnetohydrodynamics system with self-generated magnetic field terms". PhD thesis. Université de Strasbourg, 2011.

[4] G. Dakin and H. Jourdren. "High-order accurate Lagrange-remap hydrodynamic schemes on staggered Cartesian grids". *Comptes Rendus Mathematique* (2016).

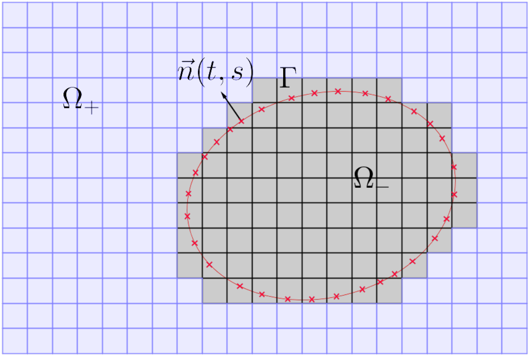

One has to define values of $\mathcal{U}$ inside the domain Ω_- denoted $\mathcal{U}_-$ using data provided on the border Γ and values inside the interior domain $\mathcal{U}_+$. Then, one builds an operator $\mathcal{R}$ such that

$$\boxed{\mathcal{R}(\mathcal{U}^+) = \mathcal{U}_-}$$

High-order accuracy interest

Here, a piston (which lies originally near $x = -1$) with infinite mass is oscillating in a gas initially at rest[5].

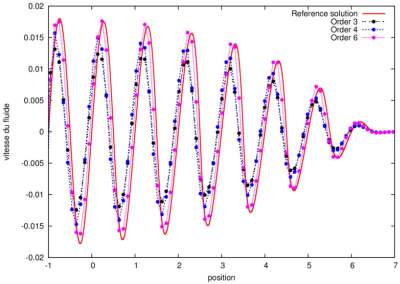

(a) High order reconstruction

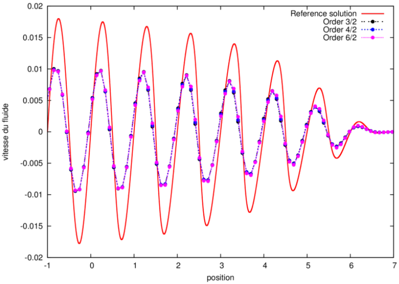

(b) Second order reconstruction

Figure : 10 cells per wavelength at $T = 9$, for order 3, 4 and 6 schemes.

[5] G. Dakin, B. Després, and S. Jaouen. "Inverse Lax-Wendroff boundary treatment for compressible Lagrange-remap hydrodynamics on Cartesian grids". *Journal of Computational Physics* (2017), pp. -.

Boundary conditions discretization for linear hyperbolic systems

Problem with initial and boundary conditions writes, for $a > 0$, $x_s = \sigma \Delta x$

$$\begin{cases} \partial_t u + a \partial_x u = 0, & t > 0,\ x > x_s, \\ u(x_s, t) = g(t), & t > 0, \\ u(x, 0) = u_0(x), & x > x_s. \end{cases} \tag{3}$$

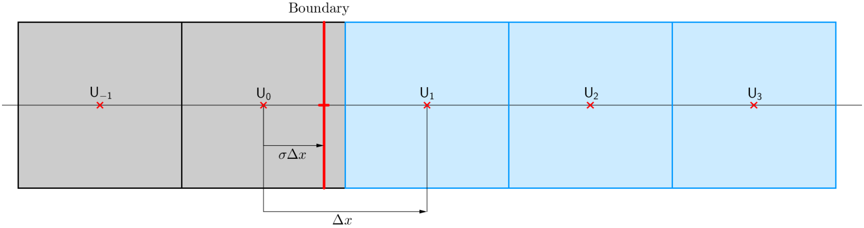

Figure : Picture of the border and fluid and fictitious domain decomposition.

The main of the inverse Lax–Wendroff procedure[6][7] is to use the following equation

$$\partial_x u = (-a)^{-1}\partial_t u, a > 0 \tag{4}$$

in order to transform spatial derivatives of u in Taylor series into time derivatives of u. Denote Δx the mesh size. The average value of u at point x in a neighborhood of x_s writes

$$\overline{u}(x,t) = \frac{1}{\Delta x}\int_{x-\frac{\Delta x}{2}}^{x+\frac{\Delta x}{2}} u(y,t)\mathrm{d}y = \frac{1}{\Delta x}\int_{x-\frac{\Delta x}{2}}^{x+\frac{\Delta x}{2}} \sum_{k\geq 0} \partial_x^k u(x_s,t)\frac{(y-x_s)^k}{k!}\mathrm{d}y. \tag{5}$$

It yields

$$\overline{u}(x,t) = \frac{1}{\Delta x}\sum_{k\geq 0} \partial_x^k u(x_s,t)\left(\frac{(x+\frac{\Delta x}{2}-x_s)^{k+1}}{k+1!} - \frac{(x-\frac{\Delta x}{2}-x_s)^{k+1}}{k+1!}\right). \tag{6}$$

[6] S. Tan and C.-W. Shu. "Inverse Lax-Wendroff procedure for numerical boundary conditions of conservation laws". *Journal of Computational Physics* 229.21 (2010), pp. 8144–8166.

[7] S. Tan and C.-W. Shu. "A high order moving boundary treatment for compressible inviscid flows". *Journal of Computational Physics* 230.15 (2011), pp. 6023–6036.

In order to simplify the notations, the following numerical coefficients are introduced

$$\psi_k(x) = \left(\frac{(x + \frac{\Delta x}{2} - x_s)^{k+1}}{k+1!} - \frac{(x - \frac{\Delta x}{2} - x_s)^{k+1}}{k+1!} \right).$$

We introduce also two parameters m and n and we write

$$\begin{aligned}
\overline{u}(x,t) &= \frac{1}{\Delta x} \sum_{k\geq 0} \partial_x^k u(x_s,t)\psi_k(x) \\
&= \frac{1}{\Delta x} \left(\sum_{0\leq k\leq n} (-a)^{-k} \partial_t^k u(x_s,t)\psi_k(x) + \sum_{k\geq n+1} \partial_x^k u(x_s,t)\psi_k(x) \right) \\
&= \frac{1}{\Delta x} \left(\sum_{0\leq k\leq n} (-a)^{-k} \partial_t^k u(x_s,t)\psi_k(x) + \sum_{n+1\leq k<m} \partial_x^k u(x_s,t)\psi_k(x) \right) + \mathcal{O}(\Delta x^m).
\end{aligned}$$

Using the fact that $u(x_s, t) = g(t)$, then we write

$$\overline{u}(x,t) = \frac{1}{\Delta x}\left(\sum_{0\leq k\leq n}(-a)^{-k}\partial_t^k g(t)\psi_k(x) + \sum_{n+1\leq k<m}\partial_x^k u(x_s,t)\psi_k(x)\right) + \mathscr{O}(\Delta x^m).$$

Consider a third oder scheme needing two ghost cells values, then dropping the $\mathscr{O}$ and taking $m = 3$, $n = 1$ it yields for $g = 0$

$$\begin{aligned}\overline{u}(x,t) &= \frac{1}{\Delta x}\partial_x^2 u(x_s,t)\left(\frac{\left(x+\dfrac{\Delta x}{2}-x_s\right)^3}{3!} - \frac{\left(x-\dfrac{\Delta x}{2}-x_s\right)^3}{3!}\right)\\ &= \partial_x^2 u(x_s,t)\left(\frac{12x^2 - 24x\sigma\Delta x + 12\Delta x^2\sigma^2 + \Delta x^2}{24}\right). \end{aligned} \tag{7}$$

Then, taking $x = x_1 = \Delta x$, it yields

$$\partial_x^2 u(x_s,t) = \left(\frac{24}{12\Delta x^2\sigma^2 - 24\sigma\Delta x^2 + 13\Delta x^2}\right)\overline{u}_1. \tag{8}$$

We can finally deduce values for $\overline{u}_0$ and $\overline{u}_{-1}$ which write

$$\begin{cases} \overline{u}_0 & = & \left(\frac{12\Delta x^2\sigma^2+\Delta x^2}{24}\right) \partial_x^2 u(x_s,t), \\ \overline{u}_{-1} & = & \left(\frac{12\Delta x^2\sigma^2+24\sigma\Delta x^2+13\Delta x^2}{24}\right) \partial_x^2 u(x_s,t). \end{cases} \quad (9)$$

We can straightforwardly rewrite those values as function of $\overline{u}_1$. It yields

$$\begin{cases} \overline{u}_0 & = & \frac{12\sigma^2+1}{12\sigma^2-24\sigma+13}\overline{u}_1, \\ \overline{u}_{-1} & = & \frac{12\sigma^2+24\sigma+13}{12\sigma^2-24\sigma+13}\overline{u}_1. \end{cases} \quad (10)$$

We generalize the reconstruction for any order m taking into account n time derivatives of g. We write the Taylor series under the matrix form

$$\begin{cases} \mathcal{U}_- = \mathcal{S}_-^n + \underline{\mathcal{Y}}_-^{m,n} \cdot \boldsymbol{\Theta}, \\ \mathcal{U}_+ = \mathcal{S}_+^n + \underline{\mathcal{Y}}_+^{m,n} \cdot \boldsymbol{\Theta}. \end{cases} \quad (11)$$

where $\mathcal{S}_-^n$ and $\mathcal{S}_+^n$ only depends on the boundary condition g. We show that the matrix $\underline{\mathcal{Y}}_+^{m,n}$ is invertible for $0 \leq n < m$ and then it yields

$$\mathcal{U}_- = \mathcal{S}_-^n + \underline{\mathcal{Y}}_-^{m,n} \cdot (\underline{\mathcal{Y}}_+^{m,n})^{-1} \cdot (\mathcal{U}_+ - \mathcal{S}_+^n). \quad (12)$$

Last, we define the reconstruction operator $\underline{\mathcal{R}}^{m,n}$ at the boundary as

$$\boxed{\underline{\mathcal{R}}^{m,n} = \underline{\mathcal{Y}}_-^{m,n} \cdot (\underline{\mathcal{Y}}_+^{m,n})^{-1}.} \quad (13)$$

N_x	$\underline{\mathcal{R}}^{3,0}$		$\underline{\mathcal{R}}^{3,1}$		$\underline{\mathcal{R}}^{3,2}$	
20	3.1e-2	·	2.8e-2	·	2.9e-2	·
40	5.9e-3	2.39	5.6e-3	2.32	5.6e-3	2.35
80	8.0e-4	2.88	7.7e-4	2.86	7.7e-4	2.86
160	1.0e-4	2.93	1.0e-4	2.92	1.0e-4	2.92

Denote $\underline{\mathcal{Z}}$ the interior numerical scheme which satisfies

$$\mathcal{U}^{k+1} = \underline{\mathcal{Z}}\mathcal{U}^{k}.$$

Let $\underline{\mathcal{R}}$ be the reconstruction operator which writes

$$\mathcal{U}_{-} = \underline{\mathcal{R}}\mathcal{U}_{+}.$$

Then the scheme writes

$$\begin{pmatrix} \mathcal{U}_{+} \\ \mathcal{U}_{-} \end{pmatrix}^{k+1} = \begin{pmatrix} \underline{\mathcal{Z}}_{1,1} & \underline{\mathcal{Z}}_{1,2} \\ \underline{\mathcal{Z}}_{2,1} & \underline{\mathcal{Z}}_{2,2} \end{pmatrix} \cdot \begin{pmatrix} \mathcal{U}_{+} \\ \mathcal{U}_{-} \end{pmatrix}^{k} = \begin{pmatrix} \left(\underline{\mathcal{Z}}_{1,1} + \underline{\mathcal{Z}}_{1,2}\underline{\mathcal{R}}\right)\mathcal{U}_{+}^{k} \\ \left(\underline{\mathcal{Z}}_{2,1} + \underline{\mathcal{Z}}_{2,2}\underline{\mathcal{R}}\right)\mathcal{U}_{+}^{k} \end{pmatrix}. \tag{14}$$

Which can be rewritten under the following form

$$\boxed{\mathcal{U}_{+}^{k+1} = \left(\underline{\mathcal{Z}}_{1,1} + \underline{\mathcal{Z}}_{1,2}\underline{\mathcal{R}}\right)\mathcal{U}_{+}^{k} = \underline{\mathcal{N}}\mathcal{U}_{+}^{k},} \tag{15}$$

where $\underline{\mathcal{N}} = \left(\underline{\mathcal{Z}}_{1,1} + \underline{\mathcal{Z}}_{1,2}\underline{\mathcal{R}}\right)$ is called the effective operator.

Denote $N_{n_c} \in \mathbb{R}^{n_c^2}, N_{n_c} = \mathcal{P}_{n_c}\mathcal{N}\mathcal{P}_{n_c}^t$ where $\mathcal{P}_{n_c}$ is the projection satisfying $\mathcal{X} \in l^2$, $\mathcal{P}_{n_c}\mathcal{X} = (X_1, ..., X_{n_c}) \in \mathbb{R}^{n_c}$. In order to avoid heavy computations introduced in GKS analysis[8], the reduced stability definition is proposed.

Definition (Reduced stability)

Let $\mathcal{Z}$ be the interior scheme and $\mathcal{R}$ be the reconstruction operator. Operator $\mathcal{N} = (\mathcal{Z}_{1,1} + \mathcal{Z}_{1,2}\mathcal{R})$ is stable in a reduced sense if

1. $\mathcal{Z}$ is proved stable for the Cauchy problem,
2. There exists $n_c \in \mathbb{N}^*$ such that $\rho(N_{n_c}) \leq 1$.

In practice, we check numerically the interior scheme stability, function of ν using von Neumann analysis[9][10] then we compute numerically the spectral radius of N_{n_c}, function of m, n, σ et ν.

[8] B. Gustafsson, H.-O. Kreiss, and A. Sundström. "Stability theory of difference approximations for mixed initial boundary value problems. II". . *Mathematics of Computation* (1972), pp. 649–686.

[9] J. G. Charney, R. Fjörtoft, and J. v. Neumann. "Numerical integration of the barotropic vorticity equation". *Tellus* 2.4 (1950), pp. 237–254.

[10] G. Allaire. *Numerical analysis and optimization: an introduction to mathematical modelling and numerical simulation*. Oxford University Press, 2007.

An instability area is observed for high values of (ν, σ) for the reconstruction operator $\underline{\mathcal{R}}^{3,0}$.

$$\underline{\mathcal{R}}^{3,0} : m = 3, n = 0 \qquad \underline{\mathcal{R}}^{3,1} : m = 3, n = 1$$

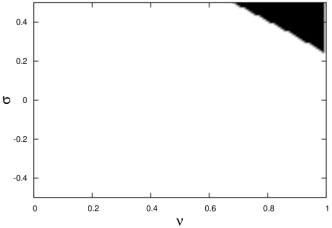

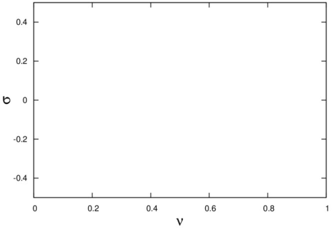

Figure : Reduced stability area $\{(\nu, \sigma) \ / \ \rho(N_{nc}) \leq 1\}$ (in white) for the third order Strang scheme with $n_c = 20$ for the reconstruction operator $\underline{\mathcal{R}}^{3,0}$ and $\underline{\mathcal{R}}^{3,1}$.

An additionnal behavior is observed here. The instability domain for $\underline{\mathcal{R}}^{4,0}$ contains an instability area for very small values of ν.

$\underline{\mathcal{R}}^{4,0} : m = 4, n = 0$

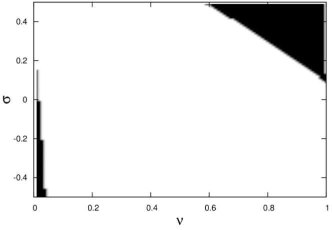

$\underline{\mathcal{R}}^{4,1} : m = 4, n = 1$

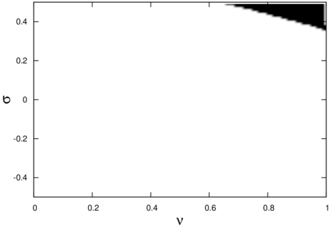

Figure : Reduced stability area $\{(\nu, \sigma) \ / \ \rho(N_{nc}) \leq 1\}$ (in white) for the fourth order Strang scheme with $n_c = 30$ for the reconstruction operator $\underline{\mathcal{R}}^{4,0}$ and $\underline{\mathcal{R}}^{4,1}$.

Instability for the O3 scheme

Here, comparisons are drawn between theoretical results and numerical ones about third order scheme using operator $\underline{\mathcal{R}}^{3,0}$ with parameters $\nu = 0.8$, $\sigma = 0.45$ and with $n_c = 200$.

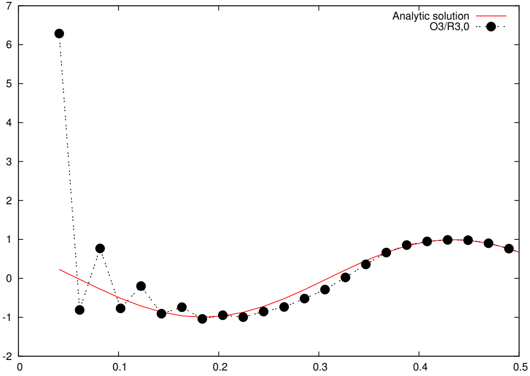

The predicted instabily in the sense of reduced stability is observed.

Instability for the P4 scheme

Here, comparisons are drawn between theoretical stability results and numerical ones about fourth order scheme using operator $\underline{\mathcal{R}}^{4,0}$ with parameters $\nu = 0.01$, $\sigma = -0.49$ and with $n_c = 30$.

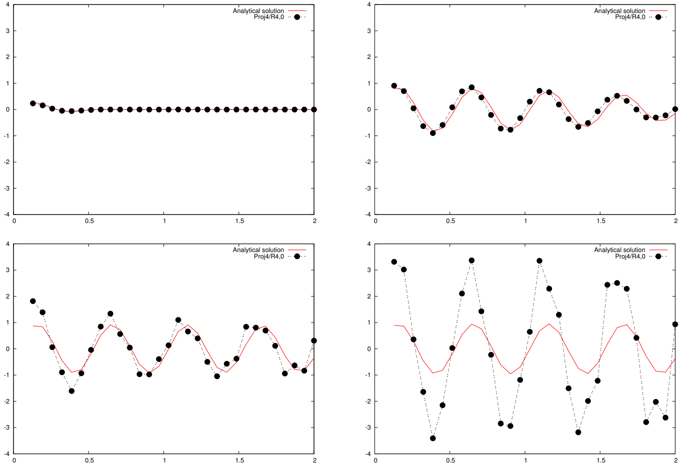

The predicted instabily in the sense of reduced stability is observed.

Boundary conditions discretization for compressible hydrodynamocs

Let $\sigma \in [-\frac{1}{2} : \frac{1}{2}[$, ΔX the grid step and $X_s = \sigma \Delta X$ a point which does not coincide with the mesh. Consider the following system

$$\left\{\begin{array}{ccc} \partial_t \rho + \partial_x (\rho u) & = & 0, \\ \partial_t (\rho u) + \partial_x \left(\rho u^2 + p\right) & = & 0, \\ \partial_t (\rho e) + \partial_x (\rho u e + p u) & = & 0, \\ p & = & EOS(\tau = 1/\rho, e, u), \\ u(x_s(t), t) & = & g(t). \end{array}\right. \tag{16}$$

Using lagrangian coordinates, it yields

$$\left\{\begin{array}{ccc} \mathrm{D}_t (\rho_0 \tau) - \partial_X u & = & 0 \\ \mathrm{D}_t (\rho_0 u) + \partial_X p & = & 0 \\ \mathrm{D}_t (\rho_0 e) + \partial_X p u & = & 0 \\ p & = & EOS(\tau = 1/\rho, e, u) \\ u(X_s, t) & = & g(t) \end{array}\right. \tag{17}$$

Matrix $\underline{\mathbf{A}} = \nabla_U F(U)$ writes for lagrangian system (17)

$$\underline{\mathbf{A}} = \begin{pmatrix} 0 & -\dfrac{1}{\rho_0} & 0 \\ \dfrac{\partial p}{\partial \rho_0 \tau} & \dfrac{\partial p}{\partial \rho_0 u} & \dfrac{\partial p}{\partial \rho_0 e} \\ u\dfrac{\partial p}{\partial \rho_0 \tau} & \dfrac{p}{\rho_0} + u\dfrac{\partial p}{\partial \rho_0 u} & u\dfrac{\partial p}{\partial \rho_0 e} \end{pmatrix}. \quad (18)$$

Obviously, matrix $\underline{\mathbf{A}}$ is not invertible. Indeed, $\underline{\mathbf{A}}$ has three eigenvalues $\lambda_1 > 0, \lambda_2 = 0, \lambda_3 = -\lambda_1$. This is an additional difficulty as in the linear analysis, hypothesis on the invertibility of A has been made.

Focus on a simple case, just to get an idea of the kind of solution we are looking for. Consider that

- $\rho_0 = 1$,
- $m = 2$, $n = 1$,
- $p = EOS(\tau, e, u) = (\gamma - 1)\frac{e - \frac{1}{2}u^2}{\tau}$.

Building the system for $\rho_0 = 1$, $m = 2$, $n = 1$

$$\left\{\begin{array}{rcl} \tau(X_s) + \partial_X \tau(X_s)(X - X_s) & = & \tau(X), \\ u(X_s) + \partial_X u(X_s)(X - X_s) & = & u(X), \\ e(X_s) + \partial_X e(X_s)(X - X_s) & = & e(X), \\ u(X_s) & = & g, \\ \partial_X \tau(X_s)\partial_\tau p(X_s) - \partial_X e(X_s)\partial_e p(X_s) - \partial_X u(X_s)\partial_u p(X_s) & = & -\mathrm{D}_t g, \end{array}\right. \tag{19}$$

whose unknowns are $\tau(X_s), \partial_X \tau(X_s), u(X_s), \partial_X u(X_s), e(X_s), \partial_X e(X_s)$.

We lack an equation to close the system. Hence, let us add another Taylor development of τ at point $X_2 \neq X_1$

$$\left\{\begin{array}{rcl} \tau(X_s) + \partial_X \tau(X_s)(X_1 - X_s) & = & \tau(X_1), \\ \tau(X_s) + \partial_X \tau(X_s)(X_2 - X_s) & = & \tau(X_2), \\ u(X_s) + \partial_X u(X_s)(X_1 - X_s) & = & u(X_1), \\ e(X_s) + \partial_X e(X_s)(X_1 - X_s) & = & e(X_1), \\ u(X_s) & = & g, \\ \partial_X \tau(X_s)\partial_\tau p(X_s) - \partial_X e(X_s)\partial_e p(X_s) - \partial_X u(X_s)\partial_u p(X_s) & = & -\mathrm{D}_t g. \end{array}\right. \tag{20}$$

Hence, we can write

$$\begin{cases} \tau_s = & \dfrac{\tau_1(X_2 - X_s) - \tau_2(X_1 - X_s)}{X_2 - X_1}, \\ \partial_X \tau_s = & \dfrac{\tau_2 - \tau_1}{X_2 - X_1}, \\ u_s = & g, \\ \partial_X u_s = & \dfrac{u_1 - g}{X_1 - X_s}, \\ e_s = & (e_1 - (X_1 - X_s)(g\partial_X u_s - \frac{\tau_s}{\gamma - 1} D_t g + \frac{-g^2}{2\tau_s}\partial_X \tau_s))(1 + (X_1 - X_s)\frac{\partial_X \tau_s}{\tau_s})^{-1} \\ \partial_X e_s = & g\partial_X u_s - \dfrac{\tau_s}{\gamma - 1} D_t g + \dfrac{e_s - \frac{g^2}{2}}{\tau_s}\partial_X \tau_s. \end{cases}$$

The system is linear. We have existence and uniqueness of the solution as far as $X_1 \neq X_s, \quad X_1 \neq X_2, \, \tau_1 \neq 0.$

$\longrightarrow$ Can we generalize this solution for any ρ_0, m and p ? For simplicity sake, we only focus on $n = 1$ reconstruction operator.

The following Lemma gives results concerning existence and uniqueness of the reconstruction in the fictitious domain[11].

Lemma (ϵ-affine EOS)

Let $m > 1$, let any ρ_0, let an ϵ-affine EOS: $p(\epsilon, \tau) = a(\tau)\epsilon + b(\tau)$. Then the system is linear. It is invertible under the condition $a(\tau_s) \neq 0$.

Examples of ϵ-affine EOS:

- Perfect gaz: $p(\epsilon, \tau) = (\gamma - 1)\frac{\epsilon}{\tau}$,
- Stiffened gas: $p(\epsilon, \tau) = (\gamma - 1)\frac{\epsilon}{\tau} - p^{\star}$,
- Mie-Grüneisen *EOS*[12]: $p(\epsilon, \tau) = p^{\star}(\tau) + \frac{\Gamma(\tau)}{\tau}(\epsilon - \epsilon^{\star}(\tau))$.

[11] G. Dakin, B. Després, and S. Jaouen. "Inverse Lax-Wendroff boundary treatment for compressible Lagrange-remap hydrodynamics on Cartesian grids". *Journal of Computational Physics* (2017), pp. -.

[12] W. B. Holzapfel. "Equations of state and thermophysical properties of solids under pressure". *High-Pressure Crystallography*. Springer, 2004, pp. 217–236.

Boundary condition discretizatio is used for the GoHy schemes[13], which are colocated high-order one-step schemes for the Euler equations.

The first test case is the Kidder isentropic compression[14] where we prescribe analytically the speed of the both side of the domain using the exact solution.

N_x	GoHy-1		GoHy-2		GoHy-3		GoHy-4		GoHy-5	
25	9.1e-4	·	3.0e-4	·	1.5e-5	·	2.0e-5	·	7.5e-6	·
50	4.5e-4	1.0	3.6e-5	3.0	5.0e-7	4.9	3.7e-7	5.7	2.9e-8	8.0
100	2.2e-4	1.0	3.0e-5	0.2	2.7e-7	0.9	1.5e-8	4.6	4.1e-10	6.1
200	1.2e-4	0.9	7.9e-6	2.0	3.0e-8	3.2	2.7e-10	5.8	2.3e-12	7.5
400	6.2e-5	0.9	2.0e-6	2.0	3.4e-9	3.2	8.5e-12	5.0	5.3e-14	5.5

Table : l^1 error in both time and space as well as experimental order of convergence for the GoHy schemes GoHy until T=0.01, with CFL=0.9. The expected order of accuracy is reached. For stability issues (predicted in the linear case), a least square method is developed for order 4 and 5.

[13] M. Wolff. "Mathematical and numerical analysis of the resistive magnetohydrodynamics system with self-generated magnetic field terms". PhD thesis. Université de Strasbourg, 2011.

[14] R. E. Kidder. *The Theory of Homogeneous Isentropic Compression and its Application to Laser Fusion*. Springer. Vol. 3B. 1974, pp. 449–464.

The Sod shock tube

The Sod test-case[15] is modified here. We consider only the right state of the initial Sod problem, with a moving wall whose speed is equal to the one of the contact discontinuity in the original problem. Thus, initial data are

$$\left\{\begin{array}{rcl} \rho(x) & = & 0.125 \\ u(x) & = & 0 \\ p(x) & = & 0.1 \\ x_l(0) & = & 0.5 \\ u(x_l(t)) & = & 0.927452624 \end{array}\right. \tag{21}$$

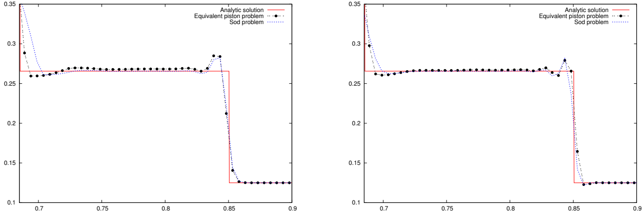

(a) Order 2

(b) Order 3

[15] G. A. Sod. “A Survey of Several Finite Difference Methods for Systems of Nonlinear Hyperbolic Conservation Laws”. *J. Comput. Physics* 27 (1978), pp. 1–31.

The border Γ is discretized using a necklace of pearls, that are represented by red crosses on the figure.

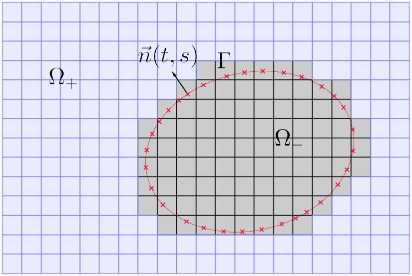

- For every pearl P_s on Γ :
  1. A stencil of points P_f in a neighborhood of P_s is built inside the fluid domain Ω_+,
  2. Using the boundary condition on P_s, the reconstruction operator is built.
- For every cell in the fictitious domain Ω_- :
  1. Find the nearest pearl P_{s_0} from the cell center,
  2. Apply the reconstruction operator.

We assess stability of the proposed reconstruction as well as their accuracy on a C^∞ test-case. In this scenario, the solid domain completely circles the fluid domain.

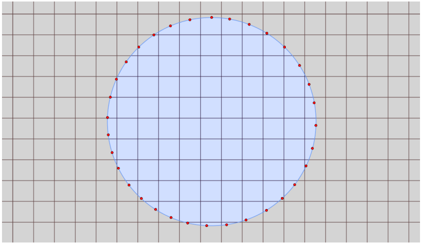

$$\begin{cases} \rho_0 &= \left(1 - \frac{(\gamma-1)\beta^2}{8\gamma\pi^2} e^{1-r^2}\right)^{\frac{1}{\gamma-1}} \\ \mathbf{u}_0 &= \frac{\beta}{2\pi} e^{\frac{1-r^2}{2}} \cdot (-y, x)^t \\ p_0 &= \rho_0^\gamma \\ \mathbf{u}\cdot\mathbf{n}_\Gamma &= 0 \end{cases}$$

N_x	GoHy-1			GoHy-2			GoHy-3		
50	4.96e-1	·	35%	5.33e-2	·	47%	9.93e-2	·	49%
100	2.52e-1	0.97	23%	1.40e-2	1.93	42%	2.04e-2	2.28	45%
200	1.20e-1	1.07	12%	4.50e-3	1.63	27%	3.46e-3	2.56	35%
400	5.66e-2	1.08	7%	1.28e-3	1.81	16%	6.43e-4	2.43	22%
800	2.74e-2	1.05	3.7%	3.23e-4	1.99	9.7%	9.31e-5	2.79	14%

Table : l^1 in both time and space on the density as well as experimental order of convergence. The cost of the inverse Lax–Wendroff procedure is given in % w.r.t the total cost of the GoHy schemes.

A incident plane wave impacts a motionless cylinder and then is scattered by the obstacle[16].

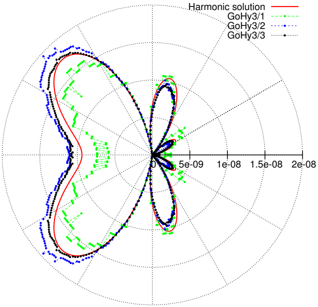

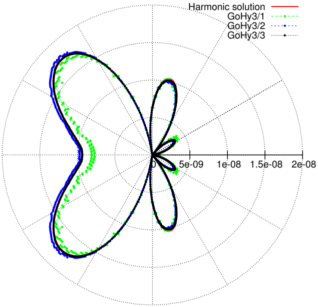

Figure : Polar plot of the pressure pertubations $\Delta p(\theta)$ on the cylinder border with respectively 20 cells per wavelength on the left and 40 cells on the right for a third order scheme, with recontructions of order 1, 2 and 3.

[16] J. J. Bowman, T. B. Senior, and P. L. Uslenghi. "Electromagnetic and acoustic scattering by simple shapes (Revised edition)". *New York, Hemisphere Publishing Corp., 1987, 747 p. 1 (1987).*

A solid wall is positionned at $(0,0)$ and has a 30° angle with respect to the horizontal axis.[17][18]. A Mach 10 shock is initialized in $\{(x,y) \in \Omega, x < -0.5\}$.

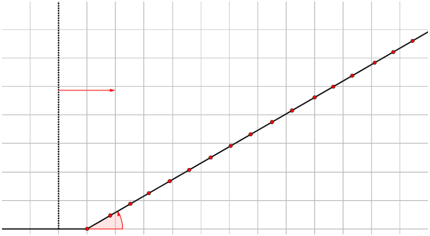

(a) Discrétisation

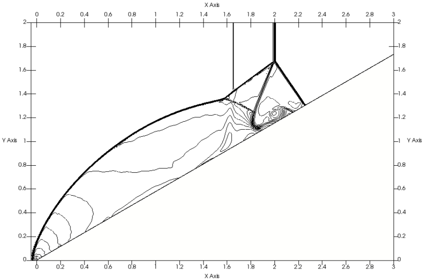

(b) Ordre 3

[17] P. Woodward and P. Colella. "The Numerical Simulation of Two-Dimensional Fluid Flow with Strong Shocks". *J. Comput. Physics* 54 (1984), pp. 115–173.

[18] S. Tan and C.-W. Shu. "Inverse Lax-Wendroff procedure for numerical boundary conditions of conservation laws". *Journal of Computational Physics* 229.21 (2010), pp. 8144–8166.

Fluid - rigid body coupling

We define the following

$$\left\{\begin{array}{rcl} M_s & = & \displaystyle\int_{\Omega_s} \rho_s(\mathbf{x})\mathrm{d}\mathbf{x} \\ \mathbf{x}_s & = & \displaystyle\frac{1}{M_s}\int_{\Omega_s} \rho_s(\mathbf{x})\mathbf{x}\mathrm{d}\mathbf{x} \\ J_s & = & \displaystyle\int_{\Omega_s} \rho_s(\mathbf{x})\|\mathbf{x}-\mathbf{x}_s\|^2\mathrm{d}\mathbf{x}. \end{array}\right. \tag{22}$$

Rigid body dynamics writes then

$$\left\{\begin{array}{rcl} M_s\mathrm{D}_t\mathbf{u}_s & = & -\displaystyle\int_{\partial\Omega_s} p\mathbf{n}\mathrm{d}S, \\ J_s\mathrm{D}_t\omega & = & -\displaystyle\int_{\partial\Omega_s} p\mathbf{n}\cdot\begin{pmatrix}-y+y_s \\ x-x_s\end{pmatrix}\mathrm{d}S, \\ \mathrm{D}_t\mathbf{x} & = & \mathbf{u}_s+\omega\begin{pmatrix}-y+y_s \\ x-x_s\end{pmatrix}. \end{array}\right. \tag{23}$$

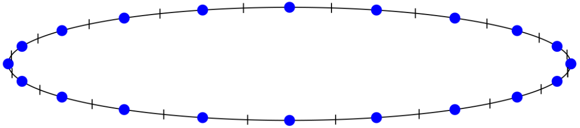

Γ is parametrized by $\gamma : [0:1] \longrightarrow \mathbb{R}^2$. Denote s the curvilinear coordinate. We have

$$\Gamma = \{\mathbf{x}, \exists s \in [0,1], \gamma(s) = \mathbf{x}\}.$$

Consider a discretization with N elements $\Gamma_{i+\frac{1}{2}}$ such that

$$\left\{\begin{array}{lcll} s_0 & = & 0, & \\ s_N & = & 1, & \\ s_{i+1} - s_i & = & \Delta s, & \forall i \in \{0, ..., N-1\}, \\ \Gamma_{i+\frac{1}{2}} & = & \{\mathbf{x}, \exists s \in [s_i, s_{i+1}], \gamma(s) = \mathbf{x}\} & \forall i \in \{0, ..., N-1\}. \end{array}\right. \tag{24}$$

The iso-Δs discretization yields spectral precision[19] for the integral of forces and torques computation on Γ. It writes

$$\int_\Gamma \phi(\mathbf{x})\mathrm{d}\mathbf{x} = \sum_{i=0}^{N-1} \int_{\Gamma_{i+\frac{1}{2}}} \phi(\mathbf{x})\mathrm{d}\mathbf{x} = \Delta s \sum_{i=0}^{N-1} \frac{1}{\Delta s} \int_{s_i}^{s_{i+1}} \phi(\gamma(s))\|\gamma\prime(s)\|ds$$

Lemma

Let Γ a closed curve smooth enough, $\phi \in \mathscr{C}^\infty$, and $\phi^\gamma_{i+\frac{1}{2}} = \phi(\gamma(s_{i+\frac{1}{2}}))\|\gamma\prime(s_{i+\frac{1}{2}})\|$. Then

$$\forall m > 0, \int_\Gamma \phi(\mathbf{x})\mathrm{d}\mathbf{x} = \Delta s \sum_{i=0}^{N-1} \phi^\gamma_{i+\frac{1}{2}} + \mathscr{O}(\Delta s^m).$$

This peculiar result has been found using traditionnal polynomial interpolation coefficients used routinely on Cartesian grids.

[19] A. Kurganov and J. Rauch. "The order of accuracy of quadrature formulae for periodic functions". *Progress in nonlinear differential equations and their applications* 78 (2009), pp. 155–159.

Coupling algorithm between fluid and structure

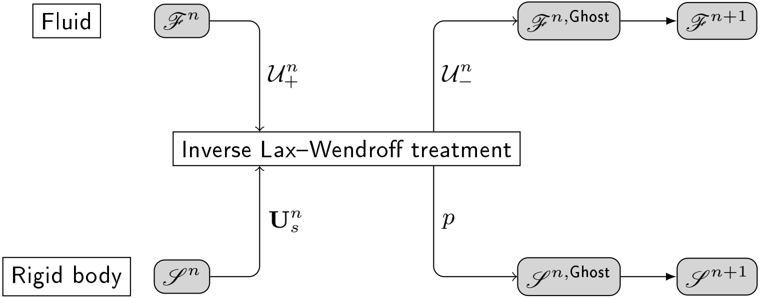

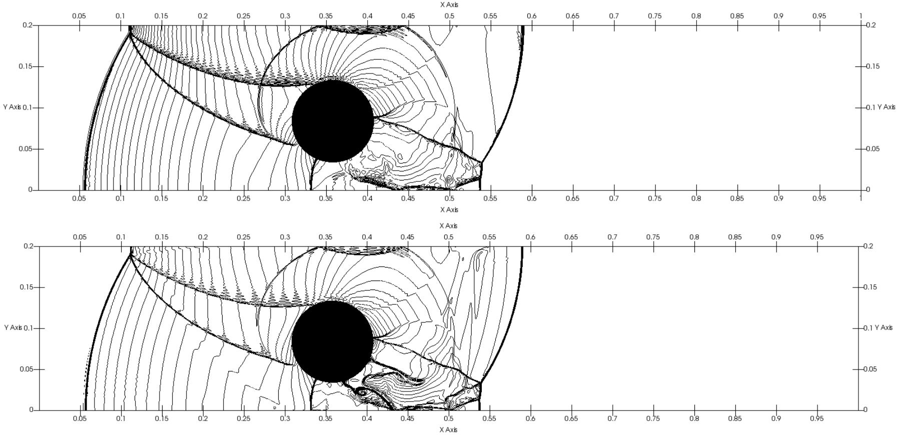

Figure : 60 pressure contours (top) from 0 to 28 and density contours (bottom) from 0 to 12 at time t=0.14 for the third order GoHy scheme with $\Delta x = \Delta y = 6.25 \times 10^{-4}$.

Fluid - rigid body interaction

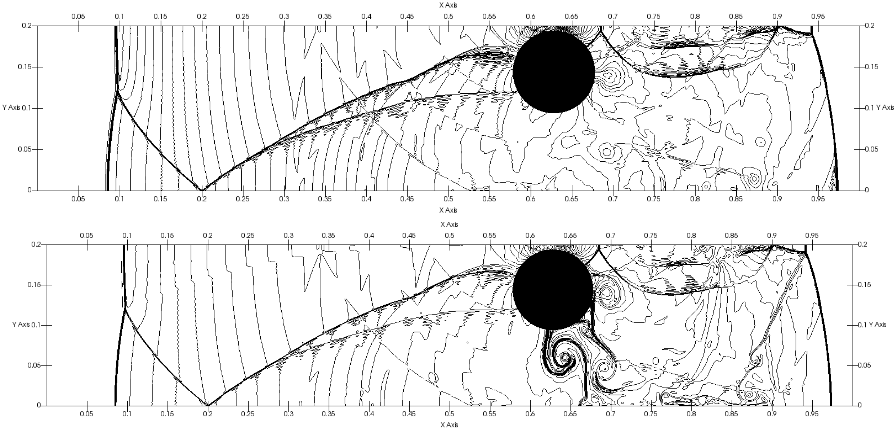

Figure : 60 pressure contours (top) from 0 to 28 and density contours (bottom) from 0 to 12 at time t=0.255 for the third order GoHy scheme with $\Delta x = \Delta y = 6.25 \times 10^{-4}$.

We present in Table 3, absolute errors made on conservation of mass and total energy which seem to converge with a slope of $0.7 - 0.8$ for the first order scheme, and near unity for the second and third order ones.

$\Delta x = \Delta y$	GoHy-1		GoHy-2		GoHy-3	
	$\|\Delta m\|$	$\|\Delta e\|$	$\|\Delta m\|$	$\|\Delta e\|$	$\|\Delta m\|$	$\|\Delta e\|$
2.5×10^{-3}	1.55e-2	4.24e-2	8.07e-3	1.71e-2	1.1e-2	2.5e-2
1.25×10^{-3}	9.41e-3	2.62e-2	4.12e-3	8.89e-3	5.58e-3	1.29e-2
6.25×10^{-4}	5.36e-3	1.54e-2	2.16e-3	4.58e-3	2.81e-3	6.47e-3
3.125×10^{-4}	2.96e-3	8.59e-3	1.11e-3	2.38e-3	1.41e-3	3.24e-3

Table : Conservation on mass and total energy at $t = 0.255$ for the lift-off cylinder test-case.

Main results

- New method for boundary conditions discretization.
- Development of a stability criterion for boundary conditions called "reduced stability".
- Straightforward coupling algorithm for fluid - rigid body interaction.

Perspectives

- 3D formulation of the boundary conditions discretization,
- Coupling between a compressible fluid and an elastic structure.
- Strong coupling using iterative method to determine both displacement and pressure forces.

Commissariat à l'énergie atomique et aux énergies alternatives
Centre de Saclay | 91191 Gif-sur-Yvette Cedex
T. +33 (0)1 69 08 66 30 | F. +33 (0)1 69 08 66 30

Établissement public à caractère industriel et commercial | RCS Paris B 775 685 019